X#Ray Lines from Gamma#Ray Bursts

X-ray Lines From Gamma-ray Bursts

Pawan Kumar

Astronomy Department, University of Texas, Austin, TX 78731

Ramesh Narayan

Dept. of Astrophysical Sciences, Princeton University, Princeton, NJ 08544

and Harvard-Smithsonian Center for Astrophysics, 60 Garden Street, Cambridge, MA 02138

pk@astro.as.utexas.edu, rnarayan@cfa.harvard.edu

ABSTRACT

X-ray lines have been recently detected in the afterglows of a few gamma-ray bursts. We derive constraints on the physical conditions in the line-emitting gas, using as an example the multiple K_α lines detected by Reeves et al. (2002) in GRB 011211. We argue that models previously discussed in the literature require either a very extreme geometry or too much mass in the line-emitting region. We propose a new model in which gamma-rays and radiation from the early x-ray afterglow are back-scattered by an electron-positron pair screen at a distance of about $10^{14} - 10^{15}$ cm from the source and irradiate the expanding outer layers of the supernova ejecta, thereby producing x-ray lines. The model suffers from fewer problems compared to previous models. It also has the advantage of requiring only a single explosion to produce both the GRB and the supernova ejecta, in contrast to most other models for the lines which require the supernova to go off days or weeks prior to the GRB. The model, however, has difficulty explaining the $> 10^{48}$ ergs of energy emitted in the x-ray lines, which requires somewhat extreme choices of model parameters. The difficulties associated with the various models are not particular to GRB 011211. They are likely to pose a problem for any GRB with x-ray lines.

Subject headings: gamma-rays: bursts – gamma-rays: theory

1. Introduction

Although much has been learned about gamma-ray busts (GRBs) in the last several years, the nature of the central exploding object remains uncertain (see Piran, 2000; van Paradijs et al. 2000; Meszaros, 2001 for recent reviews). The possible detection of x-ray lines in GRB afterglows is very important in this connection since the lines provide strong constraints on models.

Piro et al. (2000) claimed to detect an Fe K_α line and the corresponding recombination edge in GRB 991216. The line was seen about 1.5 days (in the observer frame) after the initial burst. There have been claims for iron lines also in a few other bursts (GRB 970508: Piro et al. 1999; GRB 970828: Yoshida et al. 1999; GRB 000214: Antonelli et al. 2000).

Recently, Reeves et al. (2002) reported the detection of x-ray K_α lines of Mg XI (or XII), Si XIV, S XVI, Ar XVIII and Ca XX in GRB 011211. The presence of multiple lines at apparently the same redshift makes this detection particularly interesting. If the lines are emitted isotropically, GRB 011211 must have emitted over 10^{48} ergs in each line as measured in the source frame. The emission occurred a few hours after the GRB and continued for about half an hour in the source frame. Since the lines are blue-shifted by $v/c \sim 0.1$ with respect to the GRB, the emission must have occurred within a sub-relativistic outflow from the source.

We show in this paper that it is quite challenging to come up with a viable theoretical model to explain the lines seen in GRB 011211. Recently, Borozdin & Trudolyubov (2002) have suggested that the lines may be an instrumental artifact, which would of course solve the theoretical problems. In the rest of the paper we derive constraints on some of the popular models that have been proposed so far for the line emission. The constraints apply to GRB 011211 and also to any other GRB for which a line with an energy output of about 10^{48} ergs is detected; this level of line emission roughly corresponds to the detection threshold of the current generation of instruments for a high redshift GRB. We also propose in this paper a new model for line production, which we believe suffers from fewer problems than the previous models.

Two broad classes of models have been proposed to explain the x-ray lines. In one model, it is assumed that the GRB is associated with a long-lived engine, with a duration of several hours to a day (Meszaros & Rees 2000). Part of the long-duration emission from the engine is intercepted by a funnel that has been carved out of the supernova ejecta. The intercepted radiation is reprocessed into x-ray line photons by the photoionized gas in the surface layers of the funnel. Lazzati, Ramirez-Ruiz & Rees (2002) have shown that this model is ruled out in the case of GRB 011211, the reason being that the radiation from the

central engine which causes the line emission should also be visible to the observer. There should be a very significant level of continuum radiation, which was not observed.

In the second model, it is proposed that the GRB explosion is preceded, by roughly a week or so, by a supernova explosion which ejects a dense slab of gas moving at a speed $v \sim 0.1c$. The ejected material reaches a distance $> 10^{15}$ cm by the time the GRB goes off. The x-ray photons from the GRB and early afterglow are intercepted by the slab and the radiation is reprocessed into line photons (Vietri & Stella, 1998; Vietri et al. 2001). The geometry of the outflowing gas is somewhat flexible. It could be a quasi-spherical shell, as in the model suggested by Reeves et al. (2002), or it could be in the form of a large funnel carved out in the previously ejected material. In either case, the delay of a few hours between the GRB and the line emission is explained as the geometrical time delay associated with the extra path length that photons have to travel from the GRB to the photoionized layer and then to the observer.

A third possibility, which we elaborate upon here, is that the supernova and the GRB go off simultaneously, but that the radiation from the GRB and early afterglow is scattered by a nearby scattering medium and then intercepted by the expanding surface of the supernova ejecta. The lines are produced from the surface layers of the ejecta. The time delay in this case measures the path length from the GRB to the scatterer and back to the ejecta. The basic outline of this model was briefly described by Vietri et al. (2001), who however considered the model implausible. We conclude just the opposite in this paper. We argue that, if the lines in GRB 011211 are real, they were probably produced by something resembling this model. Vietri et al. (2001) did not specify the nature of the scatterer. In our model, the scattering occurs in a pair screen created by the gamma-ray photons from the GRB. An attractive feature of the model is that the radius at which the pair screen is likely to form is close to what is needed to explain the observed time delay.

We provide some general constraints on the various models in §2 and find serious problems with all proposals. We show in §3 that the pair screen scattering model can account for the x-ray lines in GRB 011211 provided there is sufficient ambient density in the vicinity of the GRB to scatter gamma-rays to produce a significant pair screen, and provided the surface layers of the exploding star move with a significant speed $\sim 0.3c$. We conclude with a summary and discussion in §4. Some of the radiation physics relevant to line emission is discussed in the Appendix A.

2. General Constraints

Consider a photoionized medium with a radius $R = 10^{15}R_{15}$ cm as seen projected on the plane of the sky (i.e., perpendicular to the line of sight from the observer). Let the line-emitting gas have a thickness d and optical depth τ parallel to the line of sight. Let the electron density be $n_e = 10^{15}n_{15}$ cm^{-3}, the temperature be 10^7T_7 K, and let the number of electrons per Si ion be $4 \times 10^4 a_s$; we focus on Si because it is the strongest line seen in GRB 011211. The parameter a_s is defined such that $a_s = 1$ corresponds to solar composition and $a_s < 1$ corresponds to a medium in which the heavy elements are enhanced by a factor $1/a_s$.

Let the medium be irradiated by x-ray continuum radiation from the GRB for a time $t = 10^2 t_2$ s. The efficiency for converting x-ray continuum radiation (in the 1–10 keV band) to x-ray line radiation is typically a few percent under optimal conditions (Lazzati et al. 2002). Therefore, the energy in continuum irradiation is $\sim 50\zeta_{50}E_x$, where $E_x = 10^{48}E_{48}$ ergs is the energy emitted in line photons. The continuum photon number flux incident on the line producing region is thus

$$\aleph_x = \frac{50\zeta_{50}E_x}{4\pi R^2 t\epsilon_\alpha} \sim 10^{25}\frac{\zeta_{50}E_{48}}{R_{15}^2 t_2 \epsilon_3} \text{ cm}^{-2}\text{s}^{-1},$$

where $\epsilon_x = 3\epsilon_3$ keV is the energy of each line photon.

The photoionization cross-section for hydrogenic ions is $\sigma_\gamma = 7.9 \times 10^{-18} z^{-2}$ cm^2, where z is the atomic number of the line-emitting species ($z = 14$ for Si). For the photon number flux estimated above, we see that the photoionization time for Si XIII is about 3x10^{-6} s. In comparison, the recombination time for Si XIV is

$$t_{rec} \sim 5.9 \times 10^{-4}\frac{T_7^{1/2}}{z_{14}^2 n_{15}} \text{ s},$$

which, for an electron density of 10^{15} cm^{-3}, is about 10^3 times longer than the photoionization time. In the following, we therefore assume that the line emission is controlled by the recombination rate.

The rate at which Si K$_\alpha$ photons are emitted by the gas per unit projected area is

$$\dot{N}_{Si} = \frac{n_{Si}d}{t_{rec}} = \left(\frac{n_e}{4 \times 10^4 a_s}\right)\left(\frac{\tau}{\sigma_T n_e}\right)\left(\frac{z_{14}^2 n_{15}}{5.9 \times 10^{-4} T_7^{1/2}}\right)$$
$$= 6.4 \times 10^7 \frac{z_{14}^2 \tau n_e}{a_s T_7^{1/2}} \text{ cm}^{-2}\text{s}^{-1}.$$

The line flux is

$$F_{Si} = \epsilon_\alpha \dot{N}_{Si} = 3.1 \times 10^{14}\frac{z_{14}^2 \tau \epsilon_3 n_{15}}{a_s T_7^{1/2}} \text{ ergs cm}^{-2}\text{s}^{-1}. \quad (1)$$

The irradiating continuum flux in 1–10 keV photons is $F_{1-10} = 50\zeta_{50}F_{Si}$, and so the ionization parameter is

$$\xi = \frac{4\pi F_{1-10}}{n_e} = 190\frac{z_{14}^2\epsilon_3\zeta_{50}}{T_7^{1/2}}\frac{\tau}{a_s}. \quad (2)$$

For $T_7 \sim 1$, $\tau \sim 1$, $a_s \sim 0.1$ (ten times solar abundance, see Reeves et al. 2002 and Appendix A3), we find $\xi \sim 2 \times 10^3$, which is approximately the value needed for strong line emission according to Lazzati et al. (2002) for a ten times solar composition gas. Our analysis in Appendix A2 also gives a similar requirement for ξ. Thus, it appears that an optimum ionization parameter is obtained quite naturally in this problem using reasonable parameters.

Since each gas element in the medium is irradiated and emits lines for a time $10^2 t_2$ s, the total energy emitted in Si lines is

$$E_{Si} = F_{Si}\pi R^2 10^2 t_2 = 5 \times 10^{47}\frac{\xi_3 t_2 n_{15} R_{15}^2}{\zeta_{50}} \text{ ergs},$$

where we have written the answer in terms of $\xi_3 = \xi/10^3$. For an observed line energy of $10^{48}E_{48}$ ergs, we then find

$$n_{15} \sim \frac{2\zeta_{50}E_{48}}{\xi_3 t_2 R_{15}^2}. \quad (3)$$

Note that a number of parameters have disappeared from the final expression for n_e. This is because we have expressed the result in terms of the ionization parameter.

Equation (3) is an important constraint on the density of the radiating layer. The constraint applies not only to the Si line explicitly considered above, but also to lines of Fe and other elements of similar abundance when appropriate values for E_{48} and ξ_3 are substituted. As an example, for GRB 991216, Piro et al. (2000) reported the detection of an Fe K_α line with $E_{48} \sim 10$. Since the optimum ξ_3 for producing the Fe line is typically about 10 times larger than for the Si line (see Fig. 1 and also Lazzati et al. 2002), the numerical coefficient in equation (3) remains unchanged for the particular claimed Fe line.

The constraint expressed by equation (3), coupled with another constraint which comes from the observed time delay (see below), severely limits possible models for the line emission. We now consider three very different models for the line emission.

1. Shell Model: We assume that the radiating gas is in the form of a quasi-spherical shell at a radial distance $D = 10^{15}D_{15}$ cm from the GRB engine. Let the radiation from the GRB be beamed within a cone of half-angle $0.1\theta_{-1}$ radians. The observed time delay of $10^4 t_{x\gamma,4}$ s between the GRB and the X-ray lines requires

$$R_{15} = \frac{6t_{x\gamma,4}}{\theta_{-1}}, \qquad D_{15} = \frac{60t_{x\gamma,4}}{\theta_{-1}^2}. \quad (4)$$

Given this estimate of D and assuming a beaming angle of 0.1 radians, we note that a shell moving at speed $0.1c$ must have been ejected nearly a year before the GRB. The time difference may be reduced to a few days if the beam is significantly wider (Reeves et al. 2002). Substituting the above estimate of R_{15} into equation (3) we find that the mean electron density in the shell is

$$n_{15} \sim 0.06 \frac{\theta_{-1}^2 \zeta_{50} E_{48}}{\xi_3 t_2 t_{x\gamma,4}^2}, \tag{5}$$

and the thickness of the shell is

$$d = \frac{\tau}{\sigma_T n_e} = 2.7 \times 10^{10} \frac{\tau \xi_3 t_2 t_{x\gamma,4}^2}{\zeta_{50} \theta_{-1}^2 E_{48}} \text{ cm},$$

$$\frac{d}{D} = 4.5 \times 10^{-7} \frac{\tau \xi_3 t_2 t_{x\gamma,4}}{\zeta_{50} E_{48}}.$$

We consider such a small value of d/D to be highly unlikely. Because in this model the irradiation occurs on the inside of the shell and the observed line emission is from the outside, the quantity d directly measures the total thickness of the shell. Even if the shell was initially ejected with zero thickness, we estimate that thermal expansion would have broadened it considerably. For instance, if the shell was created with a temperature of 10^6 K (a conservative estimate) and it subsequently cooled adiabatically, then the relative expansion velocities of the two surfaces of the shell would be about 100 km s^{-1}, which is to be compared with the mean velocity of $0.1c$. It is unlikely that d/D would be less than the ratio of the two velocities, which gives a limit $d/D \gtrsim 3 \times 10^{-3}$, orders of magnitude larger than the value obtained in the shell model. Note that there is very little leeway in the values of the parameters τ, ξ_3, t_2, ζ_{50} and E_{48} in the expression for d/D. As discussed above, a similar constraint should apply also to the Fe line observation of Piro et al. (2000), except that the numerical coefficient is a little different because of the longer time delay in that case. We conclude that the shell model is not viable.

2. Funnel Model: We assume that the radiating layer is on the inside of a conical or quasi-cylindrical funnel with an opening angle $0.1\theta_{-1}$ radians (as viewed from the GRB engine). The estimates of R_{15}, D_{15} and n_{15} obtained in equations (4), (5) for the shell model are valid in this case as well. (Recall that R_{15} refers to the projected radius of the emitting region, and that τ refers to the optical depth parallel to the line of sight, not perpendicular to the inclined funnel surface.) In this model there is no longer any difficult with having a very small value of d/D. The ionizing photons from the GRB impinge on the inner surface of the funnel and the line photons are also emitted from the same surface. Thus, the radiating region can be an arbitrarily thin layer (unlike in the case of the shell model).

There is, however, a problem with the amount of mass required in the model. Let us assume that the funnel is carved out of a roughly quasi-spherical external medium (most probably the supernova ejecta). Given the electron density n_e and the radius of the sphere D, we estimate the external mass to be

$$M \sim \frac{4\pi}{3} D^3 n_e m_p \sim 4.3 \times 10^7 \frac{\zeta_{50} t_{x\gamma,4}}{\xi_3 t_2 \theta_{-1}^4} M_\odot.$$

For $\theta_{-1} \sim 1$, the mass is unacceptable large. Even if we take $\theta_{-1} \sim 10$, i.e., no beaming, the mass is still much too large. As in the case of the shell model, we do not have much freedom in choosing the other parameters.

One way to decrease the mass requirement in the funnel model is to enhance the density in the funnel wall relative to the rest of the ejecta. For example, one could imagine that initially there was no funnel, and that it was the GRB itself that pushed the material aside to form the funnel. It is conceivable that the material pushed aside could have piled up on the walls, giving an enhanced density there. It is not clear that this mechanism can produce the orders of magnitude density enhancement needed to reduce the mass estimate to a reasonable value.

3. Scattering Screen Model: In this model, the photoionization occurs indirectly. Photons from the GRB travel out to a screen, are scattered, and then irradiate the line-emitting gas, which is located in the surface layers of the supernova ejecta. Because the geometry is very different from the previous two models, there are two important changes. First, the time delay of 10^4 s between the GRB and the line emission measures the distance to the scattering screen ($> 10^{14}$ cm) but not the size of the line-emitting ejecta. Therefore, the estimates given in equation (4) are not valid. Instead, if we assume that the ejecta have expanded at speed $0.1c\beta_{*,-1}$ for $10^4 t_{x\gamma,4}$ s, we estimate that $R \sim D \sim 10^{13.5} t_{x\gamma,4} \beta_{*,-1}$ cm. Second, the irradiation occurs for a time $\sim 10^4 t_{x\gamma,4}$ s rather than 10^2 s, and so we expect $t_2 \sim 100 t_{x\gamma,4}$. Both changes help to ease some of the constraints.

With the above choices for R and t, we find

$$n_{15} = 20 \frac{\zeta_{50} E_{48}}{\xi_3 t_{x\gamma,4}^3 \beta_{*,-1}^2}. \tag{6}$$

The mass in the ejecta is then

$$M \sim \frac{4\pi}{3} R^3 n_e m_p \sim 2 \frac{\zeta_{50} E_{48} \beta_{*,-1}}{\xi_3} M_\odot,$$

and the kinetic energy is

$$E_{KE} \sim M(0.1c\beta_{*,-1})^2/2 = 2 \times 10^{52} \frac{\zeta_{50} E_{48} \beta_{*,-1}^3}{\xi_3} \text{ ergs}.$$

The kinetic energy may be overestimated by a factor of a few because the velocity of $0.1c$ presumably refers only to the surface layers, while the bulk of the ejecta may be moving substantially slower. Overall, the parameters are more reasonable in this model than in the previous two models. The mass and energy requirements, for instance, are consistent with an underlying supernova.

Two issues remain to be clarified in this model, both of which are discussed in §3. First, we need to identify the nature of the scattering screen. We suggest that it is a pair plasma cloud which is temporarily created by the GRB radiation itself. Second, we have to check whether there is enough scattered radiation to power the rather impressive level of line emission seen in GRB 011211.

3. X-ray Reflection from a Pair Screen

As the pulse of gamma-ray photons from a GRB moves outward, some of the photons will be scattered by electrons in their path and will collide with other outgoing photons to produce electron-positron pairs. This process has been considered by a number of authors in the context of GRBs (Thompson & Madau 2000; Meszaros et al. 2000; Beloborodov 2002; Kumar & Panaitescu 2002).

An exponential growth of pairs occurs when the optical depth for a scattered GRB photon to pair-produce off outgoing Mev photons is greater than 1. This condition gives an upper limit on the distance of the pair screen from the central explosion: $R_{\pm} \sim 10^{15} E_{52}^{1/2}$ cm. Here, E_{52} measures the isotropic equivalent energy in the gamma-ray pulse in photons of energy greater than 1 Mev, where $E_{52} \approx E_{GRB}(2m_e c^2/h\nu_p)^{-\beta}/10^{52}$ ergs, E_{GRB} is the total energy in the GRB pulse, ν_p is the frequency at the peak of the spectrum, and β is the high energy spectral index. Approximately 10^3 pairs can be created per ISM electron when conditions are right, but the number can be much less in other situations. If the optical depth of the pair screen becomes ~ 1, further pair creation is expected to be quenched and so the optical depth will not increase much above unity.

Let the medium in the vicinity of the GRB explosion be stratified with density decreasing as r^{-2}, as appropriate for a wind from the pre-supernova star: $n(r) = n_0(r/r_0)^{-2}$. For a mass loss rate of 10^{-5} yr^{-1}, which is average for a Wolf-Rayet star, and a wind speed of 10^3 km s^{-1}, the number density at a radius of 10^{15} cm is about 10^6 cm^{-3}. The optical depth in the wind is dominated by the radius at which the GRB photons are produced (where the density is highest). In the internal shock model for GRBs this radius is a $r_1 \sim$ few $\times 10^{14}$ cm. Let us assume that the pair screen forms between r_1 and an outer radius r_2. Let us

also imagine that, on average, each ISM electron produces $\eta_\pm$ pairs. The optical depth of the pair screen is then

$$\tau = n_0 \sigma_T \eta_\pm r_0^2 / r_1,$$

Assuming a mass $2m_p$ per ISM electron, the mass of the screen is

$$M = \pi \theta_j^2 2 m_p n_0 r_0^2 r_2,$$

where θ_j is the jet opening angle.

Let the pair screen move with Lorentz factor $\gamma_\pm$ as a result of absorbing momentum from the GRB photons. The momentum of the screen may be written in the form

$$P = \frac{2\pi\theta_j^2 \tau r_2 r_1 m_p c \gamma_\pm}{\sigma_T \eta_\pm}.$$

The momentum taken out of the GRB pulse is $E_{GRB} \times \min(\tau, 1)/(c\gamma_\pm^2)$, where the factor $\gamma_\pm^{-2}$ allows for the fact that, for a stationary observer, the scattered photons move at an angle of $1/\gamma_\pm$ with respect to the radial direction. Equating the momentum taken out of the GRB pulse to P we obtain an estimate for the Lorentz factor of the pair screen:

$$\gamma_\pm = \left[\frac{\sigma_T E_{GRB} \eta_\pm \min(\tau, 1)}{2\pi\theta_j^2 m_p r_2 r_1 c^2 \tau} \right]^{1/3} = \left(\frac{0.07 E_{51} \eta_\pm \min(\tau, 1)}{\theta_j^2 r_{1,15} r_{2,15} \tau} \right)^{1/3}.$$

For $E_{51} = 0.5$, $\theta_j = 0.2$, $\eta_\pm = 10$, $r_{1,15} = r_{2,15}/4 = 0.5$ and $\tau \leq 1$ we find $\gamma_\pm = 2.1$. The total energy scattered backward is about a factor of 18 less than the energy in the original GRB pulse because of Doppler de-amplification. However, the peak of the spectrum of the back-scattered radiation is a factor of ~ 4 smaller than the peak of the GRB spectrum. If the latter is at 100 kev, we expect the ejecta from the exploding star to be bathed in a radiation field with a peak at $\lesssim$25 kev, which is closer to the optimum energy for photoionizing the gas in the ejecta.

In order to have significant back-scattering of photons, τ should be close to unity. Taking $\eta_\pm = 10$, $r_0 = 10^{15}$ cm, $r_1 = 5 \times 10^{14}$ cm, this requires $n_0 \sim 7 \times 10^7$ cm^{-3}, which is substantially larger than the number density expected for a typical WR star wind. The pre-supernova star must have had an unusually heavy mass-loss rate within the last few years of its life just before the explosion.

Assuming $\tau \gtrsim 1$, the fraction of the backward scattered energy intercepted by the exploding star, assuming the ejecta are expanding uniformly with a velocity 0.15c,[1]For a spherically

expanding shell with speed v, the mean blueshift observed for a line is $2v/3$. is 6%. The intercepted flux is a factor of two larger when we include the dipole nature of Thomson scattering. Thus the total energy incident on the star is 3×10^{48} ergs. This falls short of the required amount in GRB 011211, which is $50\zeta_{50} \times 10^{48} E_{48} = 5 \times 10^{49} \zeta_{50} E_{48}$ ergs. If the supernova explosion is non-spherical, as evidenced by recent polarization observations, with the equatorial region expanding at about twice the speed of the polar region, then about 50% of the back scattered flux will be intercepted by the ejecta and the total energy incident on the expanding stellar surface is $\sim 2 \times 10^{49}$ ergs. Instead of an asymmetric supernova, we could also consider a rapidly expanding cocoon, possibly associated with the GRB jet. This will work equally well provided the density is sufficiently high (eq 6) and the transverse velocity is $\gtrsim 0.3c$.

The deceleration radius for the relativistic GRB ejecta, for the wind density deduced above, is significantly smaller than the radius r_1 of the pair screen. Thus a substantial fraction of the energy of the relativistically expanding GRB fireball will be converted to x-ray radiation before the expanding material hits the pair screen, and this energy will also be scattered by the pair screen and intercepted by the supernova ejecta. The early afterglow spectral peak is typically at an energy smaller than the GRB peak, and the peak shifts to lower energies with time as the Lorentz factor of the shock decreases. In the case of the high density surrounding medium considered here, the two emissions could have similar peak energy at early times, but the afterglow emission will subsequently shift to lower frequencies.

When we include the scattered afterglow flux, we find that the expanding supernova ejecta could receive a total of $\sim 5 \times 10^{49}$ ergs in 1–20 keV band. The afterglow radiation will be more efficient, compared to the GRB photons, in ionizing Si and other atoms which have ionization energies of a few keV. Such a continuum x-ray flux can be efficiently processed into line radiation as discussed in the Appendix, with about 2% of the continuum energy, or $\sim 10^{48}$ ergs, coming out in Si K_α photons. We note that, because of projection effects, an observer who is located in the direction of the jet will infer a factor of 2 higher line luminosity than the true isotropically averaged luminosity. This gives a safety factor of ~ 2 in the above estimates.

Because the pair cloud is moving outward with a Lorentz factor ~ 2, its optical depth is likely to reduce substantially by the time the line photons arrive at the cloud. Therefore, the x-ray lines will not be significantly attenuated by scattering off pairs. Note in addition that GRB radiation scattered off the pair cloud associated with the counter-jet is likely to be blocked by the expanding supernova ejecta (for the parameters we have considered, viz., $\theta_j = 0.2$, transverse $v/c \gtrsim 0.3$). Thus, that radiation will not contribute to the observed continuum flux.

4. Summary and Discussion

The discovery of x-ray lines in the afterglow spectra of GRBs, hours to days after the initial gamma-ray burst, poses severe problem for theoretical models. We have focused in this paper on the strong Si line observed by Reeves et al. (2002) in GRB 011211, but our arguments are valid more generally and apply, for instance, to the Fe line observed in GRB 991216 by Piro et al. (2000). In the case of GRB 011211, we have the following constraints:

1. The line-emitting gas must be moving towards the observer at an average speed of $v \sim 0.1c$ relative to the rest frame of the GRB. This suggests that the gas is associated with ejecta from a supernova explosion.

2. The time delay of $\sim 10^4$ s (measured in the source frame) between the initial GRB and the later line emission constrains the geometry of the source. In models in which the lines are produced by direct irradiation by GRB photons, the distance of the line-emitting region from the central engine (D) and the lateral extent of the irradiated region (R) are constrained by equation (4). In indirect irradiation models, in which the GRB radiation is first scattered off a nearby screen, the distance to the cloud is constrained to be $\sim 10^{14.5}$ cm and D is smaller $\sim 10^{13.5}$ cm.

3. According to Reeves et al. (2002), GRB 011211 emitted 10^{48} ergs or more in each of five K_α lines. This estimate of the energy is conservative since there might well have been additional line emission during the 11 hours between the time of the GRB and when the x-ray observations began. Regardless, the energy in the lines is a substantial fraction of the total gamma-ray energy budget of $\sim 10^{51}$ ergs (for reasonable beaming angles). Assuming the lines were produced by photoionization, the source must have been very efficient at converting continuum radiation into lines.

4. In the x-ray observations, the 1–10 keV continuum flux was found to be no more than a factor of 10 greater than the flux in each line. This introduces two constraints on models. First, the free-free emission from the gas should not be too large relative to the line emission. This requires the composition of the gas to be several times solar (Appendix A3, Reeves et al. 2002) or the temperature of the gas to be less than a keV. Second, as Lazzati et al. (2002) have argued, the photoionizing radiation from the GRB which is the cause of the line emission must not be visible to the observer. The reason is that the irradiating flux is estimated to be nearly 100 times larger than the line flux even under optimum conditions, much in excess of the observed continuum flux. This constraint eliminates all models in which the central engine puts out substantial energy for 10^4 s or longer.

5. For optimum line emission, the ionization parameter ξ has to lie in a relatively narrow range: $\xi_3 = \xi/10^3 \sim 0.1-$few. This condition introduces quite a strong constraint on the

electron density in the line-emitting gas, as shown by equation (3).

When combined together, these constraints make it very hard to find a model that can explain the lines claimed by Reeves et al. (2002) in GRB 011211. We have considered in §2 two varieties of models that have been discussed previously in the literature.

In one type of model, one has a "transmission geometry" in which the irradiation occurs on one surface of a slab of gas and the lines are emitted from the other surface. The shell model of Reeves et al. (2002) is of this type. Given the density constraint (3) and the requirement that the Thomson optical depth through the slab not be much greater than unity (in order to have any transmission at all), we deduce an impossibly thin slab at quite a large radius from the GRB engine. We believe it is extremely hard to arrange such a thin shell.

In another type of model, one has a "reflection geometry" in which both the irradiation and the line emission occur from the same surface of the line-emitting region. A good example of such a model is the funnel model discussed in §2. In this case, the high density implied by equation (3), coupled with the large length D of the funnel, imply an enormous amount of mass in the external medium. The mass can be reduced to something reasonable only by invoking highly contrived conditions.

We have also proposed and discussed in some detail a third type of model which appears to have a better chance of producing observable x-ray lines in GRBs. In this model, gamma-rays from the GRB create a pair screen temporarily at a distance of $10^{14} - 10^{15}$ cm from the central engine. The screen scatters a substantial fraction of the gamma-rays backward and thereby irradiates the expanding supernova ejecta. The lines are produced in the outer layers of the ejecta. In this model, the time delay between the GRB and the line emission reflects the added path length that the irradiating photons travel before they photoionize the line-emitting gas. The line-emitting region is significantly more compact than in the other two models. Also, each line-emitting gas element experiences irradiation for 10^4 s and not just 10^2 s as in the other models. These modifications enable this model to overcome the problems associated with the other models. Interestingly, even though irradiation occurs for 10^4 s, the model can satisfy the low continuum flux (constraint 4 above) because the irradiating photons move backwards, i.e., away from the observer. (The corresponding backward moving photons from the counter-jet are likely to be hidden by the supernova ejecta, see §3.)

The pair screen scattering model satisfies most of the constraints described above without requiring too much mass or too much energy or an implausible geometry. Moreover, the distance at which a pair screen is likely to be formed around a GRB is just what is needed to explain the observed time delay. In addition, the model has the important virtue that the

GRB and the supernova occur simultaneously. In our opinion, this is an improvement over the shell and funnel models discussed above, both of which require the supernova explosion to have occurred days to weeks before the GRB explosion.

The main problem with the pair screen scattering model is that it has difficulty explaining the total energy in the lines. Because the model involves an extra stage of scattering, the amount of irradiating flux is reduced compared to the other models. Therefore, in order to produce as much as 10^{48} ergs per line, we need (i) very efficient scattering in the pair screen, which implies order unity optical depth and a reasonably small outward Lorentz $\gamma_{\pm}$ for the pairs, and (ii) a large surface area for the supernova ejecta so that much of the reflected gamma-rays may be intercepted and reprocessed into lines. These requirements can be satisfied, as we have discussed in §3, but it requires pushing some parameters to their limit — in particular, we need a rather high mass loss rate from the pre-supernova star within a few years of the explosion, and an asymmetric supernova with a ratio of equatorial to polar velocity of about 2.

It is important to emphasize that, although we have concentrated on GRB 011211, many of the constraints we have described in this paper should be relevant for any detection of hydrogenic K_α lines of Si, Fe and other elements, in GRB afterglows. For a robust detection of a line with current instruments, the line energy has to be of order 10^{48} ergs and the continuum level has to be low, as perhaps in GRB 011211. Also, the detection is likely to be made hours to days after the initial GRB. Therefore, the problems we have emphasized with explaining the lines in GRB 011211 will carry over to line detections in other GRBs.

Acknowledgments: PK is indebted to Alin Panaitescu for valuable discussions on the physics of pair screens surrounding gamma-ray bursts, and to Gregory Shields and Craig Wheeler for numerous discussions on radiative effects, supernovae and GRBs. RN was supported in part by NSF grant AST-9820686.

Appendix A

A1. X-ray Lines from a Reflecting Slab

The flux in K_α lines of an atomic species A (Si XIV for instance) from a photoionized slab of gas is given by

$$f_\alpha = n_{A^+} n_e R_{rec} h\nu_\alpha \lambda, \tag{7}$$

where n_{A^+} is the number density of A^+ ions, $h\nu_\alpha$ is the line photon energy,

$$R_{rec} = 5.2 \times 10^{-14} z b^{1/2} \left[0.429 + 0.5 \ln b + 0.496/b^{1/3}\right]$$

is the recombination rate for hydrogenic atoms (Seaton, 1959), $b = 1.58 \times 10^5 z^2/T$ s^{-1}, and λ is the smaller of the mean free paths for ionizing photons (λ_{ion}) and line photons escaping from the region (λ_α). The two mean free paths are given by

$$\lambda_{ion}^{-1} = \sum_{i=1}^{z_A} \sigma_{ion,i}(\nu_A) n_i,$$

where $\sigma_{ion,i}(\nu_A) = 7.9 \times 10^{-18} z^{-2} (\nu_A/\nu_i)^{-3}$cm^2 is the photoionization cross-section for atomic species i at the frequency ν_A, the threshold ionization frequency for atom A, and

$$\lambda_\alpha^{-1} = \eta n_e \sigma_T + \sum_i \sigma_{ion,i}(\nu_\alpha) n_i,$$

where ν_α is the frequency of the line photon, $\eta \approx (\delta\nu/\nu_\alpha)(c/v_e)$ is the maximum allowed optical depth to Thomson scatterings such that the line broadening does not exceed the observed linewidth $\delta\nu$, and v_e is the electron thermal velocity. The ionization fraction of the atom A (assumed to be in the hydrogenic state) is determined from the following ionization equilibrium equation

$$n_{A^+} n_e R_{rec} = n_A \int d\nu \, \frac{\sigma_{ion,A}(\nu) f_\nu}{h\nu}.$$

We have solved the above equations numerically. The results are shown in Fig. 1. In the calculations, the effect of resonant line trapping was included (see the discussion in A2 below), but the Auger effect was not considered. The temperature was taken to be 10^6 K for all the calculations, and the spectrum of the illuminating x-ray continuum was taken to be $\nu^{-1.25}$. For $T = 10^7$ K, the peak of the Si line flux shifts to $\xi \sim 400$ for solar abundance and to $\xi = 2 \times 10^3$ for 10 times solar abundance, and the value of f_{Si}/f_{inc} at the peak remains nearly the same. For the Fe XXIV line, the line emission efficiency begins to decline at 2×10^3 for $T = 10^7$K. For $T = 4 \times 10^7$K our results agree with those of Lazzati et al. (2002) despite several differences in the input physics.

We discuss here an approximate analytical estimate for the line flux which provides some insight into the numerical results. Since the ionization cross-section decreases rapidly with increasing frequency, as ν^{-3}, the above equation can be written approximately as

$$n_{A^+} n_e R_{rec} \sim n_A \sigma_{ion,A}(\nu_A) f_{\nu_A}/3h \sim \frac{f_{\nu_A}}{3h\lambda_{ion,A}},$$

where $\lambda_{ion,A}^{-1} = n_A \sigma_{ion,A}(\nu_A)$ is the photo-absorption depth for photons of frequency ν_A (the threshold frequency for ionizing A). Substituting this in equation (7) we find

$$f_\alpha \approx \nu_A f_{\nu_A} \left(\frac{\nu_\alpha}{3\nu_A}\right) \left(\frac{\lambda}{\lambda_{ion,A}}\right).$$

The photoionization cross-section for Si XIV is 4×10^{-20} cm^2 or a factor of 6×10^4 larger than the Thomson cross-section. The abundance of Si, by number, for a gas of solar composition is a factor of about 3×10^4 smaller than the hydrogen abundance. Thus, λ is approximately equal to the Thomson mean free path (λ_T) for solar abundance and for an ionization fraction of $\sim 50\%$.

For small values of the ionization parameter ($\xi \lesssim 10^2$) the ionization fraction is small and the mean free path $\lambda \approx \min\{\lambda_{ion,A}, \lambda_\alpha\} \approx \lambda_\alpha$. In this case f_α/ξ increases with increasing ξ because line photons are less likely to be absorbed, as the neutral fraction of atoms of $z < z_A$ decreases with increasing ξ. Resonant line scattering makes this effect very important. At some value of $\xi \sim 10^2$, when $n_{SiXV}/n_{SiXIV} \sim 1/2$ (ionization fraction of 50%) the various mean free-paths are equal to each other and the line is most efficiently generated, i.e., f_α/ξ attains its maximum value. At larger ξ atoms are photoionized to larger depth but the line photons can only come from a smaller depth of order λ_T. Thus, f_α/ξ decreases roughly as ξ^{-1}.

The largest possible value for the line flux is $\sim \nu_\alpha f_{\nu_A}/3$. This flux is obtained under the right conditions when the abundance of A is larger by an order of magnitude than the abundances of lower atomic number elements ($z_A - 5 \lesssim z < z_a$). It is also clear that increasing the abundance of all metals, or even all neighboring z elements within $|z - z_A| \lesssim 5$, will not increase the line emission efficiency f_α/ξ since, near the maximum of f_α/ξ, λ is largely controlled by the photoionization depth, which decreases inversely with increasing abundance.

Under optimal conditions, about 5% of the 1-10 keV continuum flux can be converted to line emission. This condition is met when the peak of the incident radiation is close to ν_A and the atomic abundance of A is larger by a factor of a few than that of neighboring z-elements

A2. Resonant Line Trapping

The scattering cross-section for K_α photons of a hydrogenic atom is

$$\sigma_{21}(\nu) = \frac{c^2}{2\pi\nu_\alpha^2} \frac{1}{1 + [4\pi(\nu - \nu_\alpha)/A_{21}]^2},$$

where $A_{21} \approx 10^9 z^4$ s^{-1} is the spontaneous decay rate from $n = 2$ to $n = 1$. The mean scattering cross-section within the Doppler width of the line is $\sim A_{21}c^2/(8\pi^2\nu_\alpha^2\delta\nu_D)$. The Doppler shift is $\delta\nu_D \approx (3kT/2m_p z)^{1/2}\nu_\alpha/c = 3 \times 10^{-4} T_7^{1/2}\nu_\alpha(15/z)^{1/2}$, and therefore the scattering cross-section, within the Doppler width of the line, is $\sim 3 \times 10^{-18}$ cm^2, or two orders of magnitude larger than the photoionization cross-section. Since the photoionization

optical depth of the region from which line photons are emerging is order unity, we see that the scattering optical depth is $\sim 10^2$. Thus the probability that the K_α photons are absorbed by atoms of lower atomic number, by photoionizing them, on their way out of the line producing region is not small and must be included in the calculation of the line flux.

It is interesting to note that a K_α photon undergoes only $\sim \tau_\alpha^{2/3}$ scatterings before getting out of the trapping region (and not τ_α^2 scattering, as would be the case if the scattering cross-section was frequency independent), and the total path length traversed before escape is $\sim \tau_\alpha^{1/3}$ times the depth d of the medium. This is explained below.

In each scattering the frequency of a line photon undergoes a random walk. After N scatterings the frequency shift is given by

$$(\delta\nu/\nu_\alpha)^2 = N(v/c)^2.$$

Since the scattering cross-section for a Lorentzian profile decreases as $(A_{21}/\delta\nu)^2 \propto (c/v)^2/N$, after τ_α scatterings the cross-section decreases by a factor of τ_α. The photon then finds itself in a region with optical depth of order unity and escapes. Taking into account the distance traveled toward the surface in N scatterings, which is proportional to $N^{3/2}$, we find that photons escape after $\tau_\alpha^{2/3}$ scatterings and therefore the total path length traversed by a photon is about $\tau_\alpha^{1/3} d$ (where d is the depth of the line producing region).

When the absorption mean free path of the photon is comparable to the photoionization depth for Si atoms, the line-photon flux will be suppressed by a factor of about $\tau_\alpha^{1/3}$. For an ionization parameter of 400 and $T_7 = 0.1$, or for $\xi = 100$ and $T_7 = 1$, the two mean free paths are equal and the line flux is small. However, as we increase ξ the neutral atomic fraction decreases and the path length over which a line photon is absorbed by neutral atoms of lower atomic number goes up. An increase in the ionization parameter by a factor of four increases the photo-absorption length by a factor of four, and the emergent line emission is no longer suppressed by line trapping.

The enhanced photo-absorption of line photons due to resonant line trapping is included in the numerical results shown in Fig. 1. Our basic result is that the maximum flux in the Si XIV K_α line is a few percent of the irradiating x-ray continuum flux, and that the maximum flux is attained when $\xi \sim 10^3$ for solar composition and for $T = 10^6$K (for $T = 4 \times 10^7$K, $\xi \sim 100$ as reported in Lazzati et al., 2002). The optimum ξ increases further if the Si abundance is above solar.

A3. Bremsstrahlung Energy Loss

Let us assume that the most abundant ionic species in the plasma has an atomic number z. Its number density compared to electrons is smaller by a factor of z, and the

bremsstrahlung energy loss rate per electron in the gas is given by

$$\epsilon_B = 5.3 \times 10^{-24} n_e z T_7^{1/2} \ \mathrm{ergs\,s^{-1}}.$$

If we approximate the geometry of the region as locally plane-parallel, then the x-ray continuum flux due to bremsstrahlung is given by

$$f_B \approx \epsilon_B n_e \lambda_T = \epsilon_B / \sigma_T = 8.0 \times 10^{15} n_{15} T_7^{1/2} z \ \mathrm{ergs\,cm^{-2} s^{-1}}.$$

Comparing this with the estimate for the Si line flux given in equation (2), we find (for $z = z_{14} = \tau = \epsilon_3 = 1$)

$$\frac{f_B}{F_{Si}} \sim 26 a_s.$$

Observations of GRB 011211 indicate that the continuum flux is no more than ten times the Si line flux. This suggests that the line-emitting gas is overabundant in heavy elements by a factor of at least a few. Reeves et al. (2002) estimated an abundance of ten times solar in their analysis. Alternatively, the temperature of the gas must be less than 1 keV, so that the bulk of the bremsstrahlung emission is outside the 1–10 keV band.

The ionization parameter ξ_B corresponding to the above bremsstrahlung flux is

$$\xi_B = \frac{4\pi f_B}{n_e} = 100 T_7^{1/2} z. \tag{8}$$

For a pure H plasma this gives an ionization parameter of 100. If the ionization parameter for the incident radiation is $50\zeta_{50}$, then the bremsstrahlung flux will equal the incident x-ray flux, which is ruled out by the above-mentioned limit on the continuum flux. We need to lower the bremsstrahlung flux by a factor of about 10 to satisfy the continuum limit. From equation (8) this requires reducing the temperature to $T_7 \sim 0.1$. Lowering the temperature increases the recombination rate, and in order to get to the same ionization fraction we must increase the ionization parameter by a factor of $T_7^{-1/2}$. The upshot is that in order to get about 2-4% of the irradiating flux as Si line emission, without violating the constraint on the x-ray continuum radiation, we require the ionization parameter to be $\sim 10^3$. The argument presented in A2 also suggests $\xi \sim 10^3$ in order that K_α photons are not absorbed by atoms of lower z.

REFERENCES

Antonelli, L.A. et al. 2000, ApJ 545, L39

Beloborodov, A. 2002, ApJ 565, 808

Borozdin, K.N. & Trudolyubov, S.P. 2002, astro-ph/0205208

Kumar, P., & Panaitescu, A. 2002, in preparation

Lazzati, D., Ramirez-Ruiz, E., and Rees, M.J., 2002, astro-ph/0204319

Lazzati, D., Campana, S., and Ghisellini, G. 1999, MNRAS 304, L31

Meszaros, P. 2001, Science 291, 79

Meszaros, P., Ramirez-Ruiz, E., & Rees, M.J., 2001, ApJ 554, 660

Meszaros, P. and Rees, M.J. 2001, ApJ 556, L37

Piran, T. 2000, Phy. Rep. 333, 529

Piro, L. et al. 2000, Science 290, 955

Piro et al. 1999, Apj 514, L73

Reeves, J.N., et al. 2002, Nature 416, 512

Seaton, M.J. 1959, MNRAS 119, 81

Thompson, C., & Madau, P. 2000, ApJ 538, 105

van Paradijs, J., Kouveliotou, C., & Wijers, R.A.M. 2000, Ann. Rev. A&A 38, 379

Vietri, M., & Stella, L. 1998, ApJ 507, L45

Vietri, M., et al. 2000, ApJ 550, L43

Yoshida, A. et al. 1999, Astr. Ap. Suppl. 138, 433

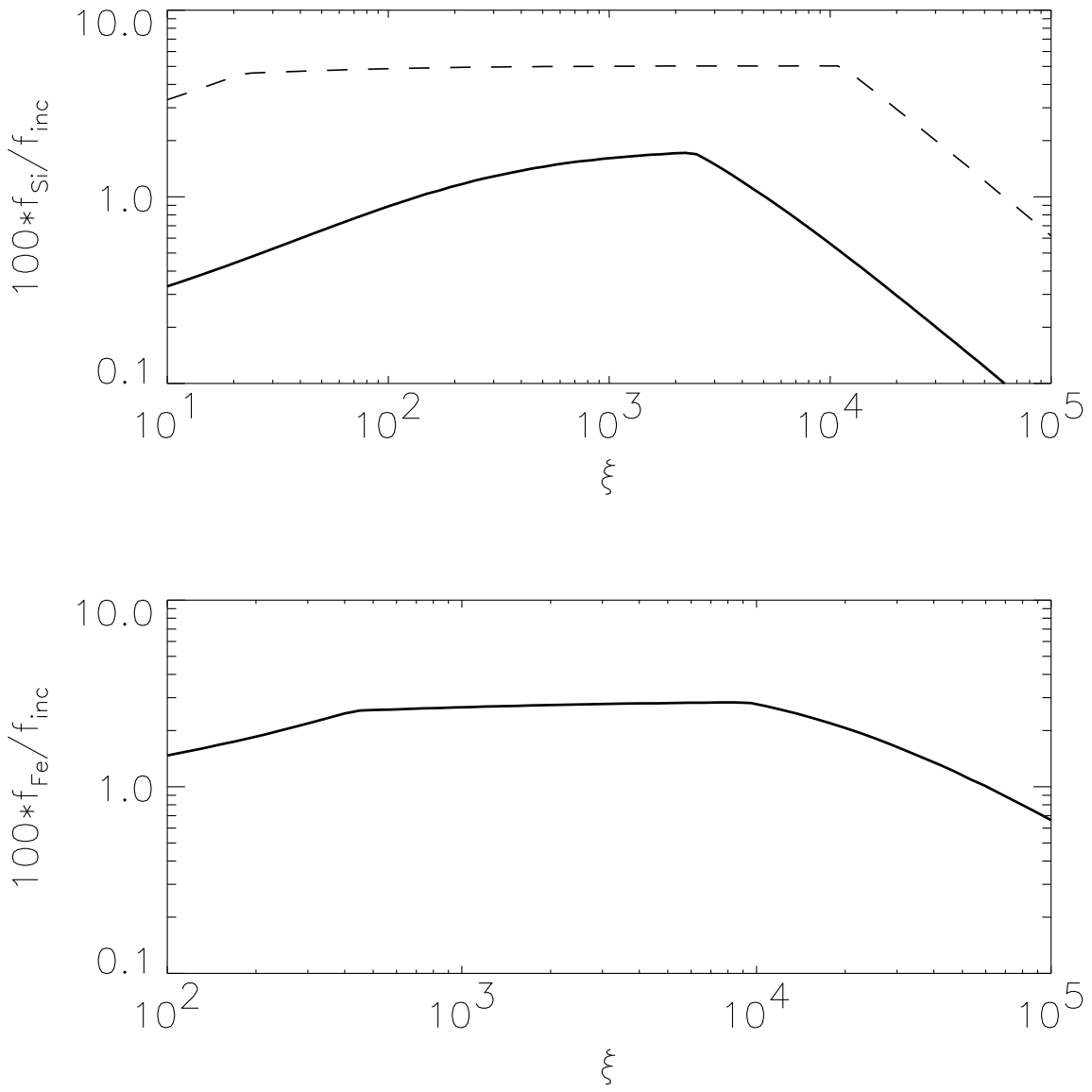

Fig. 1.— The upper panel shows the flux in the Si XIV K_α line divided by the incident flux in the 1–15 keV band as a function of the ionization parameter ξ. The solid line corresponds to solar composition and the dashed line to when the abundance of Si alone is taken to be ten times the solar value but the abundances of other elements are kept at solar. If the abundances of all metals are increased by the same factor, the curve would be similar to the solid line for $\xi \lesssim 2000$, but the decline of f_{Si}/f_{inc} at large ξ would start at a larger value of ξ (as in the corresponding results shown in Lazzati et al. 2002). The lower panel shows the flux in the Fe XXIV K_α line divided by the x-ray continuum flux.